Journal of Nuclear Materials 403 (2010) 68–74

Contents lists available at ScienceDirect

Journal of Nuclear Materials

journal homepage: www.elsevier.com/locate/jnucmat

Master curve characterization of the fracture toughness behavior in SA508 Gr.4N low alloy steels

Ki-Hyoung Lee [a,*], Min-Chul Kim [b], Bong-Sang Lee [b], Dang-Moon Wee [a]

[a] Department of Materials Science and Engineering, KAIST, Daejeon 305-701, Republic of Korea
[b] Nuclear Materials Research Division, KAERI, Daejeon 305-353, Republic of Korea

ARTICLE INFO

Article history:
Received 7 January 2010
Accepted 31 May 2010

ABSTRACT

The fracture toughness properties of the tempered martensitic SA508 Gr.4N Ni–Mo–Cr low alloy steel for reactor pressure vessels were investigated by using the master curve concept. These results were compared to those of the bainitic SA508 Gr.3 Mn–Mo–Ni low alloy steel, which is a commercial RPV material. The fracture toughness tests were conducted by 3-point bending with pre-cracked charpy (PCVN) specimens according to the ASTM E1921-09c standard method. The temperature dependency of the fracture toughness was steeper than those predicted by the standard master curve, while the bainitic SA508 Gr.3 steel fitted well with the standard prediction. In order to properly evaluate the fracture toughness of the Gr.4N steels, the exponential coefficient of the master curve equation was changed and the modified curve was applied to the fracture toughness test results of model alloys that have various chemical compositions. It was found that the modified curve provided a better description for the overall fracture toughness behavior and adequate T_0 determination for the tempered martensitic SA508 Gr.4N steels.

1. Introduction

The reactor pressure vessel (RPV) is the key component in determining the lifetime of nuclear power plants because it is subject to the significant aging phenomenon of irradiation embrittlement and there is no practical method for replacing that component. For materials used for the RPV, sufficient strength and toughness are required to prevent failure against the operating conditions and the aging degradation of materials [1,2]. Various studies have focused on improving mechanical properties by the controlling heat treatment conditions and chemical composition of conventional RPV steel, SA508 Gr.3 Mn–Mo–Ni low alloy steels [3,4]. On the other hand, some research is currently being conducted to indentify new materials with higher strength and toughness for larger capacities and longer lifetimes of the nuclear power plants. SA508 Gr.4N Ni–Mo–Cr low alloy steel, in which Ni and Cr contents are larger than conventional RPV steels, may be a candidate RPV material with the improved strength and toughness from its tempered martensitic microstructure.

The loss of toughness caused by irradiation embrittlement during reactor operation is one of the important issues for RPV materials [5–7]. The degradation of the fracture toughness results in an upward shift in the ductile–brittle transition temperature, as well as a decrease in the fracture toughness in the ductile mode [8]. In particular, the ferritic steels reveal a significant change in the fracture toughness within a small temperature range and large scatters on the measured toughness values at the same temperature [9,10]. An efficient and reliable method to quantify the embrittlement and the fracture toughness in the transition region is the master curve concept proposed by Wallin [11]. The concept was based on the 3-parameter Weibull statistics and the weakest link theory, which defines a reference temperature (T_0) to characterize the fracture toughness properties of low alloy steels in the transition temperature region. Wallin observed that the temperature dependency of fracture toughness is not sensitive to the chemical composition, heat treatment, and irradiation for ferritic steels [12,13]. This result led to the concept of a universal shape in the median toughness–temperature curve for all 'ferritic steels'. In ASTM E1921-09c, the tempered martensitic steels are considered as a class of 'ferritic steels' for which the master curve concept is applicable [14,15]. However, there are some doubts about the universal shape in the ASTM master curve for the tempered martensitic steels, such as Eurofer97 [15–17]. Furthermore, it was reported that the fracture toughness increased discontinuously when the phase fraction of the tempered martensite was over a critical fraction in the heat affected zones of SA508 Gr.3 [18]. Therefore, it may be necessary to evaluate the applicability of the master curve for the tempered martensitic SA508 Gr.4N low alloy steel.

This study focuses on the evaluation of the fracture toughness behavior with temperature for the tempered martensitic SA508 Gr.4N low alloy steels from the view point of the applicability of the standard master curve concept and statistical analysis. The results are compared with those of the bainitic SA508 Gr.3 low

* Corresponding author.
E-mail address: shirimp@kaist.ac.kr (K.-H. Lee).

0022-3115/$ - see front matter © 2010 Elsevier B.V. All rights reserved.
doi:10.1016/j.jnucmat.2010.05.029

Table 1
Chemical composition and tensile properties at room temperature of the test materials (H3:SA508-Gr.3 commercial steel, KL4 series: SA508-Gr.4N model alloys) (wt.%).

	C	Ni	Cr	Mo	Mn	P	YS (Mpa)	UTS (Mpa)	El (%)
H3	0.21	0.92	0.21	0.49	1.36	0.007	447	595	27
KL4-Ref	0.19	3.59	1.79	0.49	0.30	0.002	581	750	19
KL4-Ni1	0.22	2.66	1.81	0.54	0.33	0.002	535	698	17
KL4-Ni2	0.21	4.82	1.83	0.54	0.32	0.002	677	758	17
KL4-Cr1	0.21	3.65	1.04	0.54	0.33	0.002	585	762	17
KL4-Cr2	0.21	3.63	2.47	0.53	0.32	0.002	590	762	16
KL4-Mn1	0.21	3.64	1.85	0.54	0.11	0.002	532	712	16
KL4-Mn2	0.21	3.63	1.86	0.54	0.52	0.002	581	782	18
KL4-Mo1	0.21	3.57	1.87	0.11	0.33	0.002	533	735	17
KL4-Mo2	0.21	3.70	1.86	1.00	0.33	0.002	634	808	15
KL4-P	0.21	3.63	1.87	0.54	0.33	0.029	596	760	16
KL4-SC	0.18	3.59	1.83	0.53	0.01	0.002	583	677	15
KL4-OP3	0.21	3.60	1.78	0.49	0.20	0.002	586	743	23
KL4-OP4	0.20	2.89	1.88	0.49	0.21	0.002	575	717	23
KL4-WO	0.14	2.75	1.48	0.48	0.40	0.002	516	644	23
KL4-C	0.13	3.55	1.79	0.48	0.31	0.002	524	694	23

alloy steels. Additionally, a way to better define the fracture toughness behavior by the master curve is proposed and the result is discussed with the experimental data from various SA508 Gr.4N model alloys with different alloying contents.

2. Experimental

The materials used in this work are 15 model alloys of SA508 Gr.4N steels (KL4 series) that had various alloying element contents based on the composition range of the ASME specification [19], and H3 is an archive material of commercial SA508 Gr.3 steel used in Korean Standard Nuclear Power Plants (KSNP) [20]. Table 1 gives the chemical compositions and tensile properties of the test materials at room temperature. KL4-Ref is a reference model alloy in which the chemical composition is in the middle range of the specification of SA508 Gr.4N steel. The model alloys were all heat-treated by austenitizing at 880 °C for 2 h followed by air quenching, and were then tempered at 660 °C for 10 h, which are the typical heat treatments for RPV steels, including SA508 Gr.3.

Optical microstructures were shown in Fig. 1. Specimens were mechanically polished and etched in 3% Nital solution. The microstructures of KL4-Ref were predominantly tempered martensite, including some bainite. H3 also showed a typical tempered structure. These microstructures were composed of laths arranged in packets of up to half the prior austenite grain size. However, the lath structure of tempered martensite was more fine and complex than that of bainite. It was reported that fine Cr–carbides, such as M_7C_3 and $M_{23}C_6$, precipitated primarily in Ni–Mo–Cr steels due to higher Cr contents, while coarse M_3C type carbides were mainly observed in Mn–Mo-Ni SA508 Gr.3 steels [21].

Fracture toughness tests were carried out by 3-point bending over the temperature range from −180 to −40 °C with standard pre-cracked Charpy (PCVN) specimens (10 × 10 × 55 mm), in which the initial fatigue crack length was about 5 mm. The test temperature was maintained at ±0.5 °C by a regulated liquid nitrogen flow in an insulated chamber equipped with a proportional integral derivative (PID) controller. The test results were interpreted by following the ASTM E1921-09c in terms of the cleavage fracture toughness K_{Jc}. The K_{Jc} values obtained from the PCVN specimens were converted to the ones equivalent to the 1T-CT specimen, $K_{Jc\text{-}1T}$. The fracture toughness data were censored by the validity limit values when the measured K_{Jc} values were greater than the validity limit given by Eq. (1) according to the ASTM E1921-09c standard procedure.

$$K_{Jc\_limit} = \sqrt{\frac{b_0 \cdot \sigma_y \cdot E}{M \cdot (1-\upsilon^2)}} \tag{1}$$

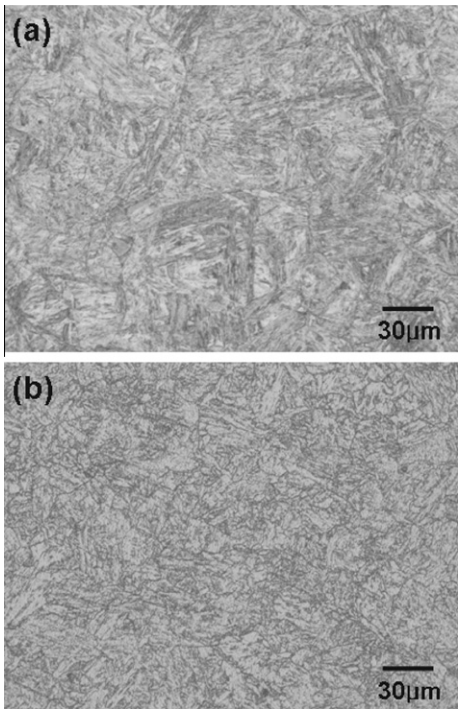

Fig. 1. OM micrographs of the model alloys: (a) KL4-Ref and (b) H3.

where b_0 is the initial ligament size, σ_y is the yield strength at the test temperature, E is the modulus of elasticity, υ is the Poisson's ratio, and M is the non-dimensional constant, which is 30 in ASTM E1921-09c.

According to the master curve concept, it is assumed that the cumulative failure probability can be calculated with the following expression by means of a 3-parameter Weibull function:

$$P_f = 1 - \exp\left[-\left(\frac{K_{Jc} - K_{min}}{K_0 - K_{min}}\right)^m\right] \tag{2}$$

where P_f is the cumulative failure probability, K_{min} is a minimum fracture toughness value, K_0 corresponds to the K_{Jc} value that represents the 63.2% cumulative failure probability, and m is a Weibull slope that defines the scatter of the K_{Jc} values on the Weibull distribution. The minimum fracture toughness of ferritic steels, K_{min} is assumed to be 20 MPa $m^{0.5}$ and the theoretical Weibull slope, m is

4. The $K_{Jc(med)}$ that corresponds to the 50% cumulative failure probability was calculated using the following equation:

$$K_{Jc(med)} = K_{min} + (K_0 - K_{min})(\ln 2)^{1/4} \quad (3)$$

The variation of $K_{Jc(med)}$ with temperature was described by using the following equation:

$$K_{Jc} = 30 + 70\exp(0.019(T - T_0)) \quad (4)$$

where T is the test temperature and T_0 is a reference temperature where the median fracture toughness of 1T specimens is equal to 100 MPa $m^{0.5}$.

3. Results

3.1. Statistical analyses of the measured fracture toughness

Fig. 2 plots the master curves in accordance with the ASTM E1921-09c standard method for 1T-adjusted 47 K_{Jc} values of KL4-Ref (a) and 59 values of H3 (b). In the case of H3, the dataset at -40 °C was excluded in determination of the reference temperature because most of the K_{Jc} values were invalid data: there were 11 invalid values and only one valid value. The upper and lower bound curves, indicating 95% and 5% failure probabilities, respectively, are also plotted by dotted lines. The reference temperature (T_0) for KL4-Ref, which was calculated from all the datasets, was −135.3 °C, which was lower than that of H3 by 57.4 °C. These results showed that the fracture toughness of the tempered martensitic SA508 Gr.4N steels is much better than the tempered bainitic SA508 Gr.3 steels in the transition temperature range.

The Weibull distribution for the measured fracture toughness of each test temperature (−140, −150, −160, −170 and −180 °C for KL4-Ref, −60, −80, and −100 °C for H3) is shown in Fig. 3. The measured toughness values are all tabulated in Appendix A. In Fig. 3, the best linear fit lines are plotted on the measured data. The low slope implies a large scatter of data including the increased K_{Jc} values due to constraint loss at that temperature. According to Wallin [9] and Anderson and Stienstra [22], the theoretical Weibull slope of the fracture toughness data would be over 4, which was derived from the crack tip stress–strain distribution. If the slope is much less than four at the test temperatures, it is thought that the constraint loss may have extensively affected the measured K_{Jc} values and the dataset should be censored carefully for evaluation of the cleavage fracture toughness.

Fig. 4 shows the Weibull slope of the dataset at each test temperature. The temperature scale was normalized by the reference temperatures (T_0) of the tested materials. The ASTM E1921-09c mentioned that the applicability range of the fracture toughness data for determining a master curve is T_0 ±50 °C. The datasets of

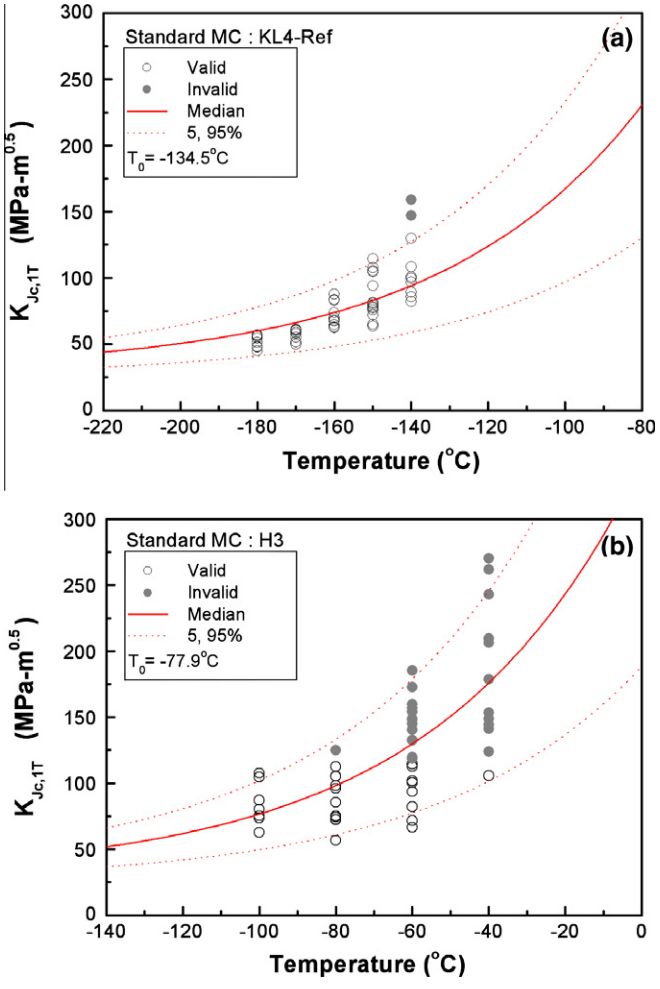

Fig. 2. Standard ASTM E1921-09c master curves and the measured fracture toughness values of (a) KL4-Ref and (b) H3 (the invalid points were determined using ASTM E1921 validity limit equation (Eq. (1)). There were no ductile crack).

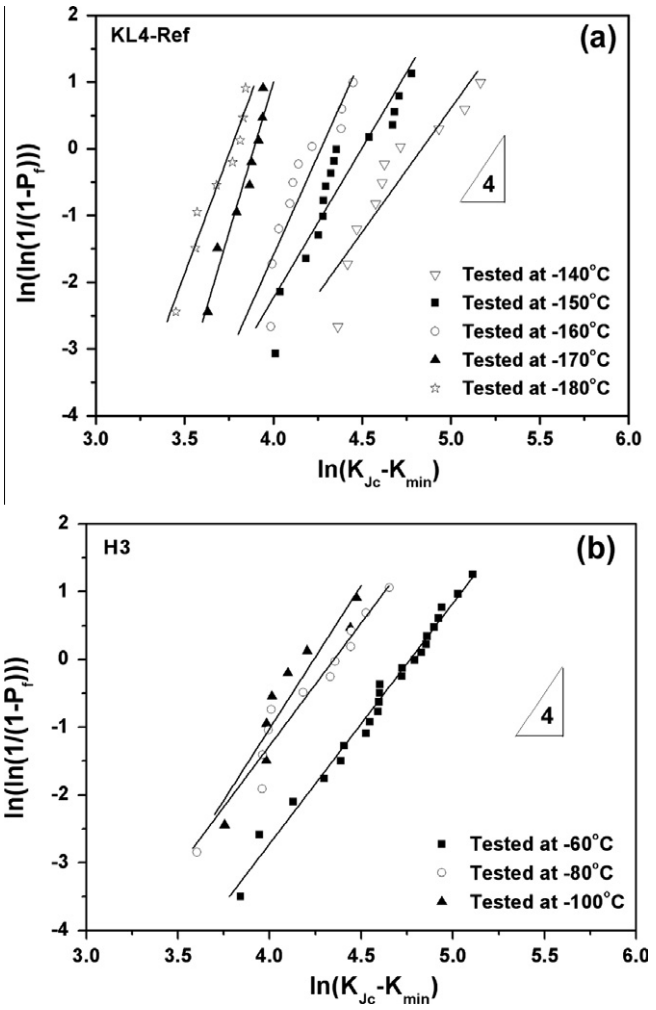

Fig. 3. Statistical distributions of the fracture toughness values determined from the 3-parameter Weibull function for (a) KL4-Ref and (b) H3.

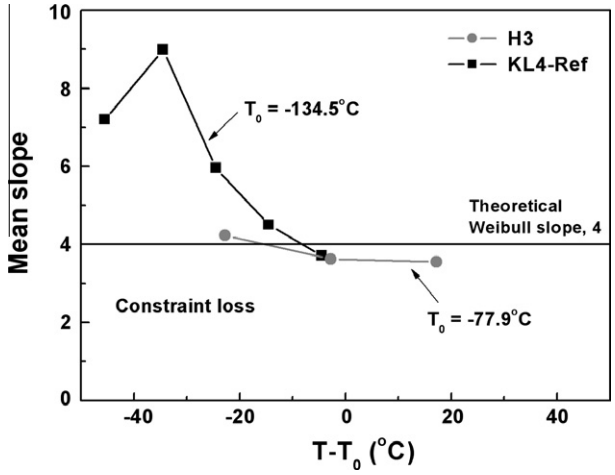

Fig. 4. Weibull slopes for dataset at each test temperature.

the KL4-Ref at each test temperature produced Wiebull slopes ranging from 3.71–8.99. The slopes for the datasets of H3 ranged from 3.55–4.23. The slopes clearly tended to decrease with a rise of the test temperature in both steels. However, the changes in the slopes of the H3 datasets were not extensive within the broad normalized temperature range from −23 °C to 18 °C, while those of KL4-Ref changed rapidly in a narrow range from −35 °C to −5 °C. In particular, the comparatively high slopes of datasets for KL4-Ref were observed, indicating an extremely small scatter of the measured fracture toughness values in low test temperatures. Surely, the size of the dataset has a strong effect on the variability of the slope on a Weibull plot [23,24]. The small datasets were subject to large uncertainties, while the median slope for the large datasets tended to be close to the theoretical value of 4. Wallin proposed that a permissible range of slopes for datasets, including about 10 specimens, would be between 2.2 and 7.5 based on the enormous data filed [24]. Considering these results, the Weibull slopes for the datasets of both KL4-Ref and H3 were approximately within the predicted range, especially in the case of H3, but the result of KL4-Ref at low temperature, −170 °C, was outside the predicted range.

3.2. Fracture toughness behavior with temperature

In Fig. 2b, the data distribution of H3 was well fitted to the master curve shape throughout the whole temperature range, even with the K_{Jc} values over the validity limit at high temperature such as −40 °C. However, Fig. 2a shows that, at the low test temperatures (−170 and −180 °C), all values are located below the median curve. On the contrary, the dataset at a high temperature of −140 °C deviated from the upper region of the median curve. Therefore, the dependency of the K_{Jc} values on the temperature in KL4-Ref was thought to be steeper than that predicted by the standard master curve in tested temperature region.

In order to assess the influence of the data distribution on the T_0 determination, the T_0 obtained from all the data was compared with the T_0 values calculated from each single-temperature dataset. Fig. 5 gives the single-temperature T_0 determination results with standard deviations for KL4-Ref (a) and H3 (b), respectively. Although the number of data points measured at −180 °C for KL4-Ref was insufficient for valid T_0 determinations, the datasets were included in analyses in order to confirm the general tendencies of T_0 variations. The standard deviations for T_0 were calculated according to the formula given in ASTM E1921-09c:

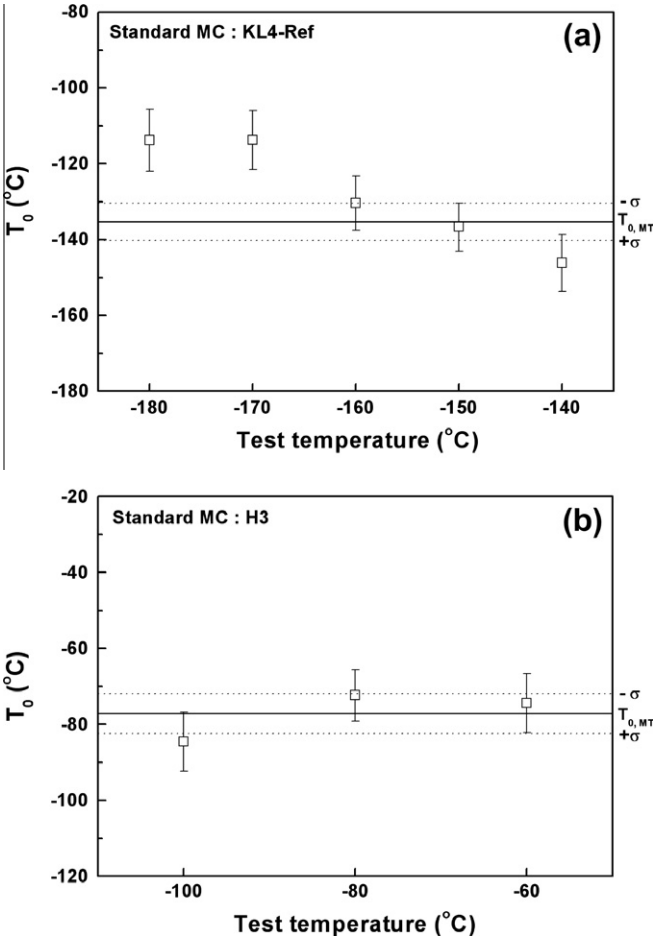

Fig. 5. T_0 values calculated from the single-temperature datasets in (a) KL4-Ref and (b) H3.

$$\sigma = \sqrt{\frac{\beta^2}{r} + \sigma_{\exp}^2} \tag{5}$$

where β is the sample size uncertainty factor given in Table 2, r is the total number of valid specimens, and $\sigma_{\exp}$ is the contribution of experimental uncertainties, $\sigma_{\exp}$ = 4 °C. The $K^{eq}_{Jc(med)}$, an equivalent value of the median toughness for a dataset, is defined as follows [25]:

$$K^{eq}_{Jc(med)} = \frac{1}{r}\sum_{i=1}^{r} 30 + 70\exp(0.019(T_i - T_0)) \tag{6}$$

where r is the total number of valid tests and T_i is the individual test temperature. According to the results of H3, the maximum difference between the T_0 values from each dataset was about 12 °C. The T_0 values from each dataset deviated only 7 °C from the T_0 that was determined from all the datasets. Considering the standard deviation of each T_0 value, all individual T_0 values overlapped with the average T_0 from all the data. However, in the case of KL4-Ref, the

Table 2
Values of the parameter β according to ASTM E1921-09c, as function of the equivalent median toughness.

$K^{eq}_{Jc(med)}$ (Mpa m^{05})	β (°C)
>83	18
83–66	18.8
65–58	20.1

differences among the T_0 values from individual single-temperature datasets were large, where the maximum difference was 37.9 °C. Standard deviations did not overlap with $\pm 1\sigma$ lines of T_0 from all the data, in particular, at the low temperatures of −180 and −170 °C. The T_0 values determined by the single-temperature analysis of the standard master curve method decreased with a rise in the test temperature. These results may have arisen from the steeper dependence of the K_{Jc} values on the temperature, which was mentioned in the previous paragraph. Hence, we attempted to modify the master curve expression in order to more accurately describe the fracture toughness behavior for tempered martensitic SA508 Gr.4N steels.

4. Discussions

4.1. Adjustment of the master curve expression

It has generally been theoretically and experimentally reported that the major microstructural factors affecting the fracture toughness of steels are grain size and distribution of second phases, such as carbide and inclusion. However, Shin et al. reported that the relationships between grain size or carbide size and fracture toughness did not fit well with the general tendency in the case of steels with a predominantly tempered martensite microstructure [18]. Lucon [17] also raised doubts about the applicability of the standard master curve concept to the ferritic/martensitic steels with chromium contents between 9% and 12%. Thereafter, Bonade et al. [16] and Muller et al. [15] attempted to modify the standard master curve expression for the tempered martensitic Eurofer97 steel.

In this sense, in order to evaluate the fracture toughness behavior of the tempered martensitic KL4-Ref alloy accurately, modifying the curve shape was attempted in the same way as in previous research [15–17]. The adjustment of the master curve equation was undertaken to more accurately describe the K_{Jc} evolution. The exponent of the master curve equation was re-determined from the exponential fitting for datasets of KL4-Ref:

$$K_{Jc(med)} = 30 + 70\exp(0.033(T - T_0)) \quad (7)$$

where the exponential parameter related to the curve shape was changed from 0.019 to 0.033 for the standard master curve expression. To minimize changes in the basic form of the master curve expression, only the exponential coefficient related to the curve shape was adjusted, while the other parameters (30 and 70) related to the position of the curve on the temperature axis were not adjusted [25]. Fig. 6 shows the curve with the adjusted exponential coefficient on the plot of K_{Jc} values obtained from KL4-Ref. The standard master curve is also plotted in Fig. 6. The T_0 that was determined from the new curve expression was −142.2 °C, which is lower than the T_0 calculated from the standard master curve expression by 7.7 °C. As can be observed, the new curve shape provided a much better description for the datasets throughout the all test temperature. Additionally, the shape of the tolerance-bounds was also adjusted according to the new expression so that it predicted the distribution of data scatter properly.

In order to check the consistency of the adjusted curve for evaluating the fracture toughness, the T_0 values obtained from the single-temperature determination procedure at each test temperature were compared with the T_0 calculated from all datasets by a multi-temperature determination procedure. Fig. 7 summarizes the results obtained by the modified master curve equation. In contrast to the results obtained by the standard master curve (Fig. 5a), the T_0 values determined at each temperature slightly deviated from each other and also from the T_0 value by using the multi-temperature procedure with all datasets. Therefore, the adjusted curve

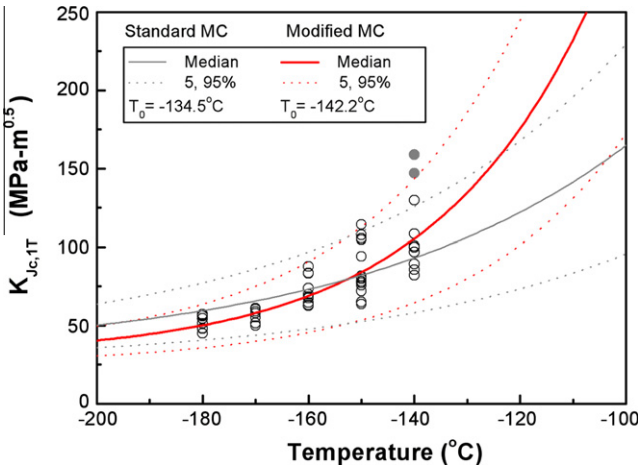

Fig. 6. A curve with an adjusted exponential parameter and the measured fracture toughness values of KL4-Ref.

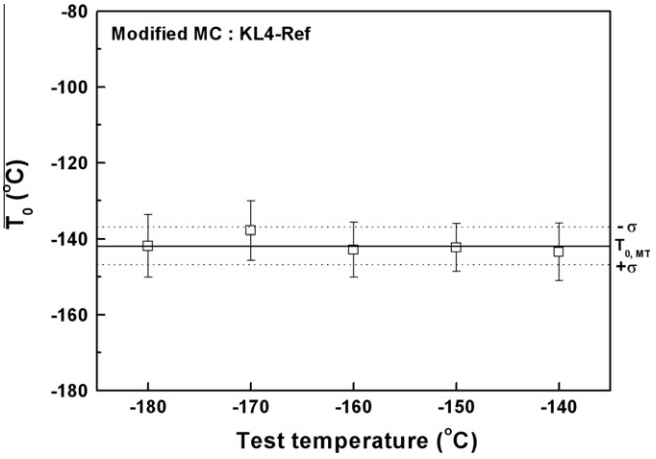

Fig. 7. T_0 values from determined from adjusted curve expression for the single-temperature datasets in KL4-Ref.

expression may be more suitable to evaluate the reference temperature of the fracture toughness in the lower transition region for the tempered martensite steels.

Some researchers mentioned that the constraint loss from small specimens such as PCVN may result in the steeper transition of the measured fracture toughness [26–28]. They explained that the constraint limit of the current standard method may not be conservative. In the current study, the valid data were mainly located within the lower transition region where the test temperatures are lower than T_0, due to the specimen size limit for validity in the higher temperature region. Therefore, testing programs with bigger specimens would be necessary for ensuring that the steeper master curve is valid in the whole transition region including higher temperatures than T_0.

4.2. Application to other model alloys

We tried to confirm that the adjusted curve shape represents the overall fracture toughness behaviors of other model alloys with different chemical compositions. Fig. 8 shows the standard and the adjusted curve plots for the measured K_{Jc} values obtained from 15 different model alloys, where the temperature scale was normalized by the T_0 values of each alloy listed in Table 3. The invalid K_{Jc} values in Fig. 8 did not contain stable crack growth data and

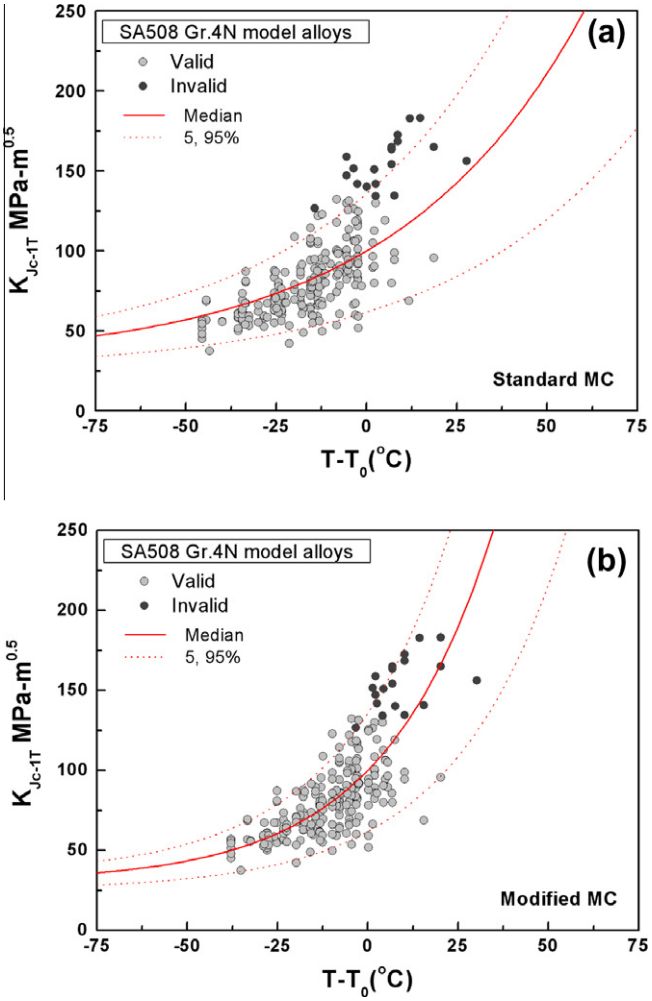

Fig. 8. Measured K_{Jc} values of the KL4 model alloys with (a) the standard master curve and (b) the modified curve.

Table 3
T_0 values of model alloys determined by the standard master curve and the modified curve.

Alloy	Standard T_0 (°C)	Adjusted T_0 (°C)
KL4-Ref	−134.5	−142.2
KL4-Ni1	−106.8	−114.2
KL4-Ni2	−161.8	−166.7
KL4-Cr1	−75.7	−86.7
KL4-Cr2	−161.8	−165.5
KL4-Mn1	−142.5	−144.1
KL4-Mn2	−137.5	−142.6
KL4-Mo1	−136.5	−141.4
KL4-Mo2	−120.1	−127.6
KL4-P	−104.9	−110.2
KL4-SC	−155.1	−157.5
KL4-OP3	−132.1	−134.4
KL4-OP4	−127.0	−126.8
KL4-WO	−97.7	−100.2
KL4-C	−138.7	−140.2

those were all determined using ASTM E1921 validity limit equation, Eq. (1). These invalid values may be too high due to loss of constraint from small PCVN specimens. Bigger specimens may be useful to enlarge the valid data range.

The adjusted curve expression described the temperature dependency of the K_{Jc} values more properly. The number of data points above and below the median curve was counted for the standard and adjusted curve, respectively. These results are presented in Table 4. In the case of the standard master curve plot, the proportions of data points below and above the median curve were 60% and 40%, respectively. In particular, in the lower transition region where the test temperatures were below T_0 −20 °C, most of the measured K_{Jc} values were smaller than the median fracture toughness line. These results mean that the data distribution was asymmetric for predicting the standard master curve. In contrast, a considerable agreement was found for the adjusted curve where the proportions of data below and above the median were almost the same (52% and 48%). As a result, the adjusted curve expression provided improvements in the description of the fracture toughness behavior of the tempered martensitic SA508 Gr.4N steels. Based on the current investigation as well as others, it is believed that the modified curve with an adjusted exponential coefficient can provide a good description of the K_{Jc} evolution with temperature and an accurate determination of T_0 for tempered martensitic SA508 Gr.4N Ni–Mo–Cr low alloy steels.

Table 4
Distribution of data points according to the standard and adjusted curve concept.

	Number of K_{Jc} below median curve	Number of K_{Jc} above median curve	Number of K_{Jc} out of the tolerance-bounds
Standard MC	152	99	30
Adjusted MC	131	120	21

5. Conclusion

The fracture toughness behavior of the tempered martensitic SA508 Gr.4N Ni–Mo–Cr low alloy steels was characterized and compared with that of bainitic SA508 Gr.3 by using the master curve concept in the transition region. The main findings are as follows.

1. The Weibull plots showed that the data distribution for the Gr.3 steel was approximately within the theoretically predicted range. However, the datasets for the Gr.4N model showed had comparatively higher slopes, which mean smaller scatters of the measured fracture toughness data in low test temperatures.
2. For K_{Jc} evolution with temperature, the data of Gr.3 steel fitted well to the standard master curve shape. However, the measured K_{Jc} values of the Gr.4N model alloys change more steeply with temperature than those predicted by the standard master curve concept.
3. A modified curve with the adjusted exponent adjusted from 0.019 to 0.033, better describes the steeper K_{Jc} evolution throughout the test temperature range for the tempered martensitic low alloy steels. T_0 values could be consistently determined at different test temperatures by using the modified curve in the single-temperature analysis procedure.

Acknowledgement

This work was supported by the Nuclear Research & Development of the Korea Institute of Energy Technology Evaluation and Planning (KETEP) grant funded by the Korea government Ministry of Knowledge Economy.

Appendix A

The measured K_{Jc} values and crack lengths for tested specimens (The invalid points were determined using ASTM E1921 validity limit equation (Eq. (1)). There were no ductile crack growths).

Alloy	Test temp. (°C)	Adj. to 1T – K_{Jc} (Mpa $m^{0.5}$)	a/W
KL4-Ref	−140	82.1, 85.6, 89.2, 96.9, 99.8, 100.7, 108.4, 129.8, 147.0*, 158.9*	0.524, 0.525, 0.524, 0.523, 0.526, 0.523, 0.523, 0.526, 0.526, 0.522
	−150	63.7, 64.9, 72.0, 75.7, 77.2, 77.3, 78.1, 79.8, 80.8, 81.6,94.1, 104.6, 105.5, 107.7114.3	0.522, 0.523, 0.528, 0.524, 0.523, 0.526, 0.520, 0.527, 0.523, 0.527, 0.525, 0.526, 0.521, 0.524, 0.521
	−160	62.6, 63.0, 64.6, 67.5, 68.3, 69.8, 73.8, 83.3, 83.6, 87.7	0.518, 0.526, 0.522, 0.520, 0.525, 0.528, 0.520, 0.526, 0.530, 0.523
	−170	49.9, 51.5, 55.1, 57.8, 58.9, 60.5, 60.8, 61.0	0.528, 0.523, 0.521, 0.524, 0.525, 0.526, 0.522, 0.523
	−180	45.0,47.9,48.1,51.4, 54.4, 55.9, 56.4, 57.0	0.523, 0.521, 0.522, 0.526, 0.520, 0.518, 0.525, 0.522
H3	−40	105.7, 123.8*, 141.2* 144.2*, 148.7*, 153.5*, 178.8*, 206.5*, 209.6*, 242.9*, 261.8*, 270.4*	0.495, 0.506, 0.525, 0.506, 0.480, 0.499, 0.522, 0.531, 0.524, 0.500, 0.529, 0.524
	−60	64.6, 66.6, 71.6, 82.1, 93.5, 100.5, 101.9, 112.5, 114.4118.5*, 119.0*, 119.5*, 119.6*, 132.4*, 132.7*, 140.5*, 144.9*, 148.1*, 148.8*, 154.0*, 157.1*, 159.8*, 172.7*, 185.3*	0.502, 0.510, 0.513, 0.498, 0.552, 0.504, 0.509, 0.515, 0.516, 0.518, 0.514, 0.506, 0.526, 0.506, 0.503, 0.520, 0.537, 0.526, 0.522, 0.506, 0.523, 0.520, 0.509, 0.516
	−80	72.4, 72.6, 74.2, 75.1, 85.5, 96.0, 98.1, 105.1, 112.5, 125.0*	0.504, 0.503, 0.509, 0.506, 0.511,0.516,0.499,0.510, 0.512, 0.510
	−100	62.7, 73.6, 73.7, 75.3, 80.3, 87.0, 104.7, 107.7	0.518, 0.512, 0.499, 0.508, 0.492, 0.501, 0.505, 0.510

References

[1] S.G. Druce, B.C. Edwards, Nucl. Energy 9 (1980) 347.
[2] K. Suzuki, J. Nucl. Mater. 108&109 (1982) 443.
[3] Y.S. Ahn, H.D. Kim, T.S. Byun, Y.J. Oh, G.M. Kim, J.H. Hong, Nucl. Eng. Des. 194 (1999) 161.
[4] Y.R. Im, Y.J. Oh, B.J. Lee, J.H. Hong, H.C. Lee, J. Nucl. Mater. 297 (2001) 138.
[5] B.S. Lee, M.C. Kim, M.W. Kim, J.H. Yoon, J.H. Hong, Int. J. Press. Ves. Piping 85 (2008) 593.
[6] G.Z. Wang, J.H. Chen, Metall. Mater. Trans. 27A (1996) 1909.
[7] G.R. Odette, Scr. Metall. 17 (1983) 1183.
[8] P. Spätig, R. Bonadé, G.R. Odette, J.W. Rensman, E.N. Campitelli, P. Mueller, J. Nucl. Mater. 367–370 (2007) 527.
[9] K. Wallin, Eng. Fract. Mech. 19 (1984) 1085.
[10] K. Wallin, Eng. Fract. Mech. 22 (1985) 149.
[11] K. Wallin, Int. J. Mater. Prod. Technol. 14 (1999) 342.
[12] K. Wallin, T. Saario, K. Törrönen, Met. Sci. 18 (1984) 13.
[13] K. Wallin, Int. J. Press. Ves. Piping 55 (1993) 61.
[14] Standard Test Method for Determination of Reference Temperature, T_0, for Ferritic Steels in the Transition Range, E1921-09c, ASTM International, 2009.
[15] P. Mueller, P. Spätig, R. Bonade, G.R. Odette, D. Gragg, J. Nucl. Mater. 386–388 (2009) 323.
[16] R. Bonade, P. Spätig, N. Baluc, J. Nucl. Mater. 367–370 (2007) 581.
[17] E. Lucon, J. Nucl. Meter. 367–370 (2007) 575.
[18] H.S. Shin, J.H. Kim, J.H. Hong, J.G. Moon, I.S. Chung, J. Korean Inst. Met. & Mater. 37 (1999) 1260.
[19] Standard Specification for Quenched and Tempered Vaccum-treated Carbon and Alloy Steel Forgings for Pressure Vessls, A 508/A 508M-05b, ASTM International, 2005.
[20] B.S. Lee, W.H. Yang, M.Y. Huh, J.H. Kim, J.H. Hong, Trans. KSME A 24 (2000) 303.
[21] S.G. Park, M.C. Kim, B.S. Lee, D.M. Wee, J. Korean Inst. Met. & Mater. 46 (2008) 771.
[22] T.L. Anderson, D. Stienstra, J. Test. Eval. 17 (1989) 46.
[23] R. Bouchard, G. Shen, W.R. Tyson, Eng. Fract. Mech. 75 (2008) 3735.
[24] J.G. Merkle, K. Wallin, D.E. McCabe, NUREG/CR-5504, ORNL/TM-13631, US Nuclear Regulatory Commission, November 1998.
[25] E. Lucon, M. Scibetta, E.V. Walle, Int. J. Fract. 119 (2003) 161.
[26] J.A. Joyce, R.L. Tregoning, Eng. Fract. Mech. 72 (2005) 1559.
[27] H.J. Rathbun, G.R. Odette, T. Yamamoto, G.E. Lucas, Eng. Fract. Mech. 73 (2006) 134.
[28] P. Mueller, P. Spätig, J. Nucl. Mater. 389 (2009) 377.